Pergamon

Int. Comm. Heat Mass Transfer, Vol. 27, No. 2, pp. 191–200, 2000
Copyright © 2000 Elsevier Science Ltd
Printed in the USA. All rights reserved
0735-1933/00/$–see front matter

PII S0735-1933(00)00100-7

FLOW VISUALIZATION AND PRELIMINARY MEASUREMENTS OF A CONFINED JET WITH AND WITHOUT TARGET

L. P. Chua, S.C.M. Yu and H-S. Li
School of Mechanical & Production Engineering,
Nanyang Technological University,
Nanyang Avenue, Singapore 639798
E-Mail: mlpchua@ntu.edu.sg

(Communicated by J.P. Hartnett and W.J. Minkowycz)

ABSTRACT

Flow visualization using smoke in a confined jet with and without a target has been investigated in the paper. The results indicated that there are flow oscillations in the confined jet with and without the target. The results also confirm the existence of re-circulation flow when the flow hit the back wall and causing the mean velocity profiles did not reach the zero values at the far end of transverse locations. The flow visualization provides useful qualitative information about the flow physic of the fluidic flowmeter.

© 2000 Elsevier Science Ltd

Introduction

One of the many engineering applications of the confined jet is to use as fluidic flowmeter for flow measurement. The fluidic flowmeter makes use of hydrodynamic oscillation of the fluid for the determination of flow rates. In these devices, oscillatory flow is created whereby the frequency of the oscillations (which can be easily sensed by appropriate sensors) is directly proportional to the flow rate. Furthermore, they are also insensitive to calibration of physical properties of the fluid and have no moving mechanical parts.

Some of the commonly used methods to cause the required flow oscillations are relaxation and feedback oscillators. Honda & Yamasaki [1] proposed a flowmeter that consisted of a main nozzle and target, which was derived from feedback oscillator type fluidic flowmeter by eliminating both sidewalls

based on a topological isomorphism between fluidic and vortex flowmeters. The purpose of the target was to improve the oscillation sensitivity at the lower limit.

The objective of this project is to investigate the flow characteristics of the confined jet through flow visualization; in particular the development of the jet issuing from a rectangular nozzle of aspect ratio 6.0 into a confined chamber, of fixed given geometry with and without a rectangular target inserted. Pictures and measurements were taken for two Reynolds numbers, 5517 and 2759 respectively (corresponding to jet exit velocity U_j=20 m/s and 10 m/s) and the placing of a bluff body (a rectangular target of 24x20x10 mm) at a distance of 81.5 mm from the exit. Note that the geometry of the present jet is the same as that developed by [2].

Experimental Arrangements

Atmospheric air was drawn into the confined test chamber through a 19-mm internal diameter pipe by using a three-phase oilless regenerative blower (see Figure 1). Using a frequency converter, which directly controlled the electrical power input to the blower, regulated the blower speed. Inlet air flow to the test chamber was first passed through a 900 mm long pipe with a flow straightener which was made of drinking straws (ϕ3mm x 90mm long) placed at the entrance. Two wire meshes were secured at both ends of the straightener in order to break down the turbulence. The rectangular nozzle, which formed by 2 perspex plates with rounded leading edges. The linear relationship between the motor speed and the jet velocity was calibrated using a Pitot-static tube connected to a twin-wire resistance-probe water manometer with a resolution of 0.01mm water. To facilitate the discussion, the side where the nozzle is situated, is hereafter referred to as the front wall and the direct opposite side where the 19 mm diameter exit pipe is located is referred to as the back wall. The two 500x280 mm^2 perspex sheets that sandwiched the rectangular frame are referred to as the sidewalls.

A Panasonic Digital Still Camera, NV-DCF1EN, mounted on a Fotomate tripod was used to capture images of the flow. The camera was placed 500 mm directly in front of the chamber. Black cloths to prevent reflections on the plastic chamber wall covered both the camera and the tripod. Two table-lamps with the top making an angle of 30° to the sidewall were also used to light up the confined chamber. To enable the flow to be viewed by naked eyes, smoke that was generated by a smoke generator RG-100, was injected into the jet. The RG-100 is a smoke generator developed for laboratory use and ventilation testing. To avoid over generating the smoke that will turn into oil and dirty the test rig, the smoke

generator was only operating 50% of its capacity. The smoke generated was enough to be captured by the digital camera.

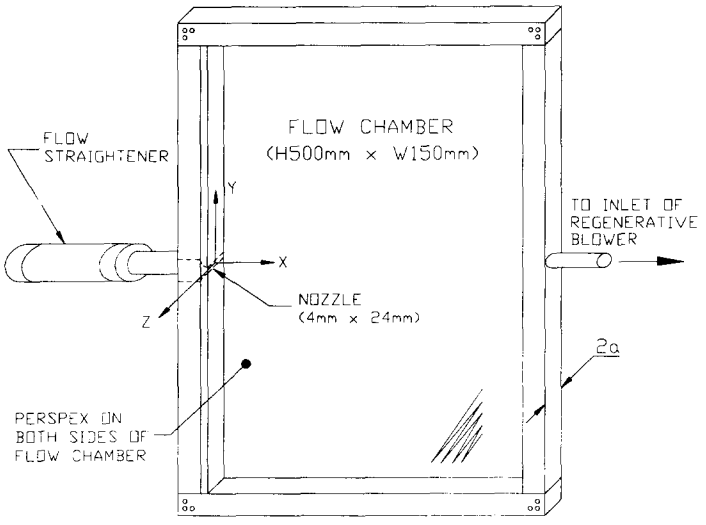

FIG. 1

A Schematic sketch of the confined jet

Mean velocity was measured in the confined jet with and without the target using hot-wire ($\phi 5\mu m$, Pt-10%Rh, Wollaston, length $\approx$ 1.0mm) operated with the constant temperature anemometer made in-house, at an overheat ratio of 1.6. As the rectangular nozzle is rather small, the linear relationship between the motor speed and the jet velocity was first calibrated using a Pitot-static tube. The hot wire was then calibrated at the potential core with the known motor speed and subsequently the jet velocity. The calibration constants of the hot-wire were determined by method of least squares. Signals from the hot wire and the manometer were digitized by a 12 bit analog-to-digital converter and subsequently processed by a computer. A sample of 999 was taken (duration = 3 sec) for each data set used for processing. For the flow visualization, the blower was allowed to run for a short period of time to allow the flow to be stabilized before smoke was injected into the chamber.

Results and Discussion

Figures 2a and b are the flow visualization of the confined jet without the presence of a target for Reynolds numbers of 2759 and 5517 respectively. The flow is from left to right in Figure 2 (It is also the same for Figure 4). It can be observed in Figure 2a that the confined jet was approximately symmetric about the centerline at different downstream position of the nozzle. The potential core of the jet was continually consumed by turbulent mixing layers whilst the jet progressively widened and spreading out like wedge-shape. As the flow approaches the back wall, it converges toward the exit. As the exit area is not big enough for all the jet to exit at the same time, the flow hit the back wall and bounced back, resulting in re-circulation. This back-flow motion was just clear enough to be viewed by naked eyes but could not be captured by the camera. The flow was left to continue for some time and the smoke particles could be observed outside the wedge-shape jet boundary. Although not visible enough to be captured by camera, it indicated the back-flow. The air outside the boundary of the wedge-shape jet was not totally static; instead it had certain velocity due to the back-flow. Figure 3a shows the normalized velocity profiles at different streamwise location, it can be seen that unlike the conventional jet issuing into the stagnation environment [3,4], the tail of the profiles never reached zero at high y/L position. Note that L is the location where the mean velocity, U resumes half of the centerline maximum velocity, U_0. The profiles confirm the existence of back flow through the measurement by using hot-wire [5].

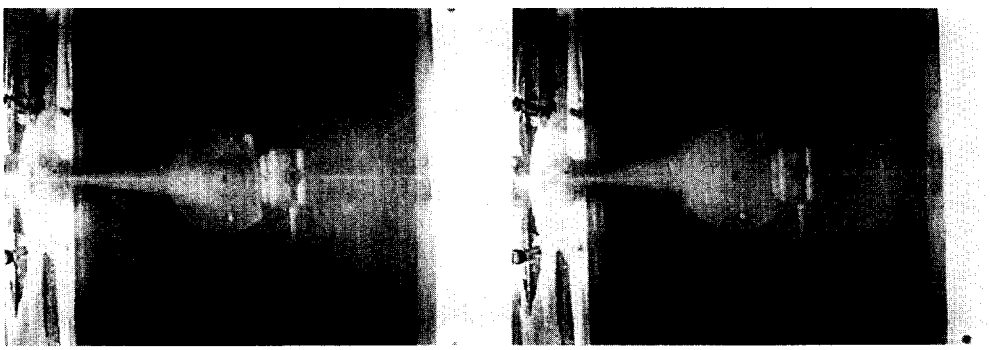

(a) (b)

FIG. 2

Flow visualization of the confined jet without target (a) Re=2759 and (b) Re=5517

Figure 2b shows that the confined jet was again symmetric about the centerline at different downstream position of the nozzle and spread out with a wider wedge angle than that of Re=2759 in the

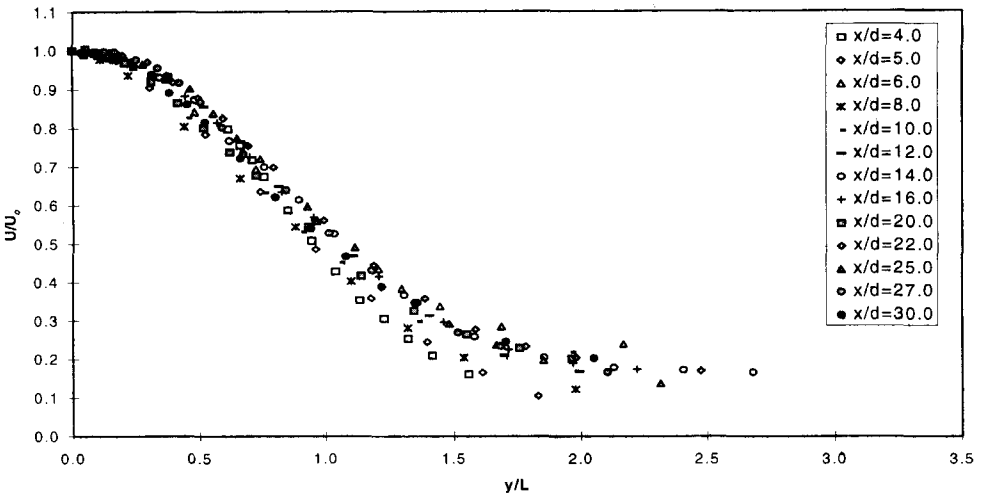

(a)

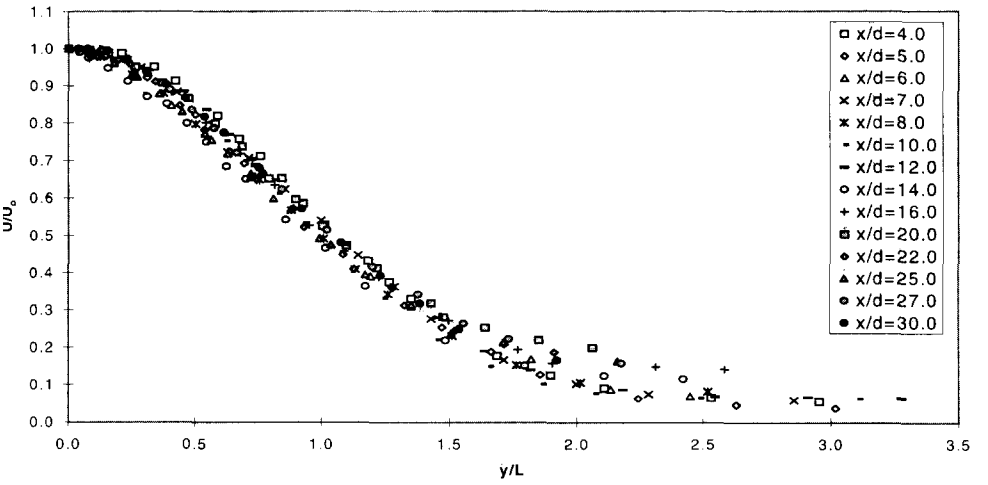

(b)

FIG. 3

Mean velocity distributions for (a) U_j =20m/s and (b) U_j =10m/s without target

near field. As the suction at the exit is much stronger, the jet is not as developed as in the U_j=10m/s case and started to converge at about 45mm from the exit located at the back wall. This distance was about double as compared to the Re=2759 case of 22mm. The experiment was allowed to continue until smoke particles were seen outside the wedge-shape and it took more than twice the time than that of the low Reynolds number. Figure 3b showed that the velocity profiles are not reached zero at high y/L locations. However, the magnitudes of U/U_0 at high y/L locations in Figure 3b are smaller than those for U_j=10 m/s. These could be due to the stronger suction at exit for U_j=20m/s, resulted in less air being left for re-circulation. Further, as the air hit harder at the back wall, the momentum loss should be greater and the re-circulated air are comparatively weaker and consequently resulted with lower velocity distribution at high y/L.

For the flow visualization of the confined jet with target at Re=2759 as shown in Figure 4a, the jet at the beginning, as in Figure 2a without target, spread out in a wedge-shape manner. As the jet hit the target, it dispersed but followed closely the contour of the target and continued its motion to the exit. It could be observed in Figure 4a that more smoke was concentrating at the surroundings of the target. This indicated that the motion of the air at these areas was not moving as fast as other portion of the jet. The wedge-shape of the jet contour was observed not as symmetric with the centerline as compared with the jet without target. These may be due to the flip-flop nature of the fluidic flowmeter, resulted in less well-defined wedge contour. Figure 5 shows the velocity profiles before the target for U_j=10m/s. Figure 5 again indicates that the velocity are not zero at high y/L locations due to the back-flow. It can also be

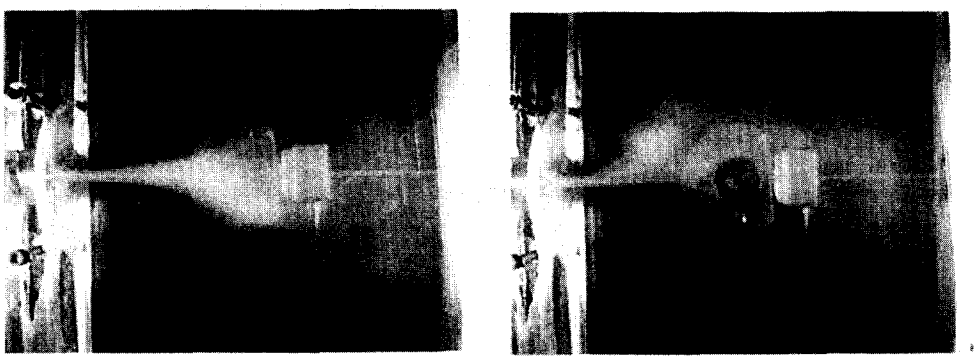

(a) (b)

FIG. 4

Flow visualization of the confined jet with target (a) Re=2759 and (b) Re=5517

observed in the Figure that the U/U_0 can reach the value of 0.3 (for x/d=16), which is much higher than the value of 0.2 for the jet without target (see Figure 3a). The target has thus enhanced the recirculation and oscillation of the confined jet.

Figure 4b shows the visualization of the confined jet with target at Re=5517. The jet showed no well-defined wedge-shape as in the previous three cases. However it can be observed at the beginning of the flow, the jet flow out the nozzle, hit the target, it rebounded and dispersed to the sides of the target. The flow continued and then converged towards the exit (at the back wall) as Re=2759. There is a special phenomenon in this case that the smoke tends to concentrate above the centerline before the target but not distributed evenly as in the other flow conditions described earlier. As the measured velocity profiles

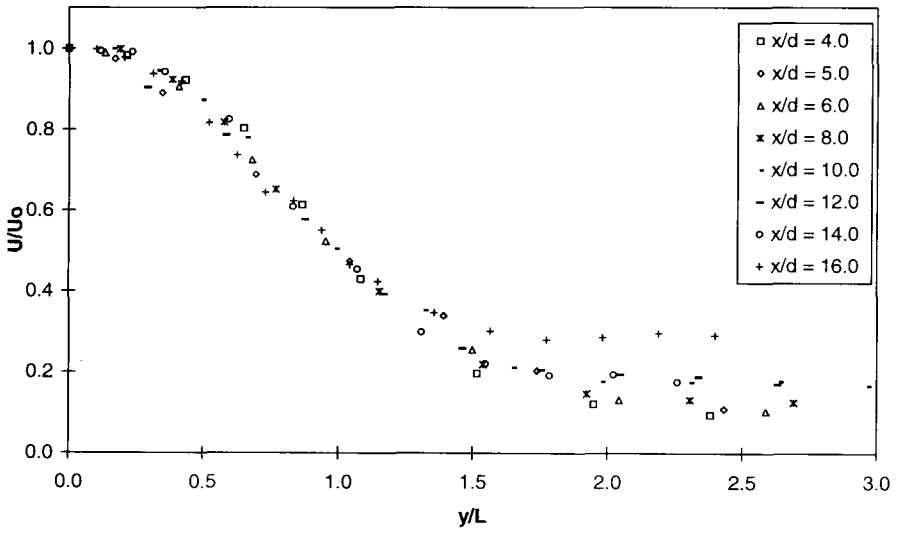

FIG. 5

Mean velocity distributions at 4.0<x/d<16.0 for Uj=10m/s

before the target (not shown here) are similar to Figure 5, and indicate no obvious bias distributions of the velocity contributed at the positive y direction. It is difficult to explain the phenomenon initially, however, it is later found out that there is slight leakage at the bottom of the confined chamber due to prolong used of the test section. As the test section is under the suction of the regenerative blower, the pressure inside the chamber is smaller than the ambient atmospheric pressure, a slight leakage at the bottom will end up with the higher pressure air is pushing the jet to the upper test section. The chamber now is under repaired and better photograph should be able to obtain.

Figures 6a and b show the velocity distributions of $U_j = 20m/s$ and $10m/s$ respectively at two streamwise locations after the target. Note that the target was located at $x/d = 20.375$ and extended $10mm$ in the streamwise direction. It can be observed from Figure 6a (also 6b) that at $x/d = 25$ for

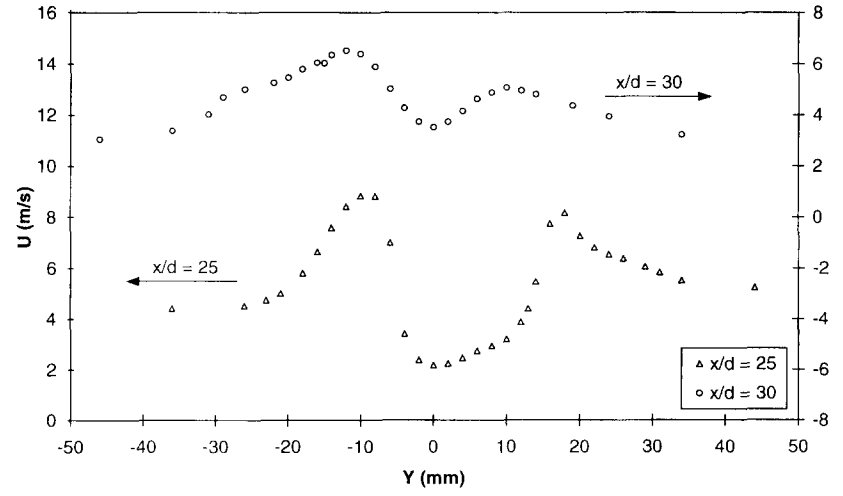

(a)

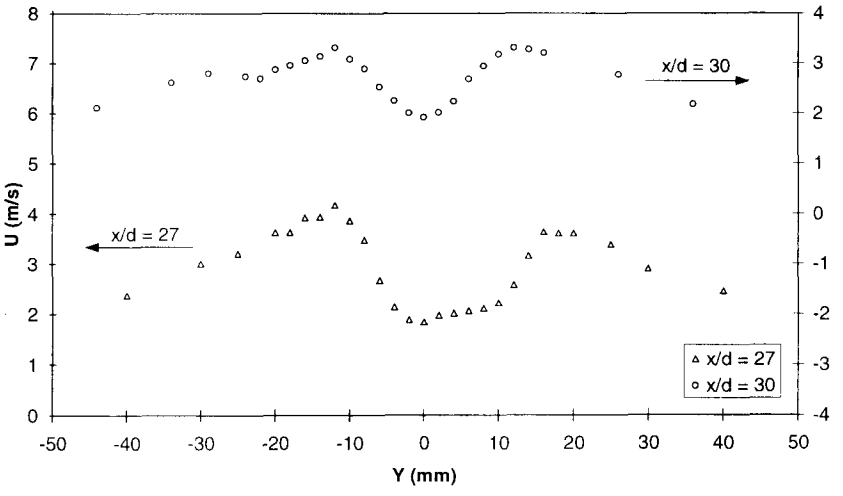

(b)

FIG. 6

Distributions of mean velocity profiles after the target for (a) $U_j = 20m/s$ and (b) $U_j = 10m/s$

U_j=20m/s (also at $x/d = 27$ for $U_j = 10m/s$), the velocity distribution is not only in the shape of a combination of jet and wake flows, but also skews towards the positive y locations. The shape of the velocity profiles obtained suggested that the velocity might still be in the transient state to a perfect combination of jet and wake velocity profiles at such close distances of about $2d$ to $4d$ behind the target. The skewness suggests that the jet was oscillating about the target. It can also be observed in Figures 6a and b that the velocity shapes at $x/d = 30$ $U_j = 20m/s$ and $10m/s$ respectively resemble more of a smooth combination of jet and wake profiles with the latter exhibiting better symmetry about the centerline. However, due to the limitation of the hot-wire probe, it is impossible to take further downstream profiles without disturbing the flow at the exit [5,6].

Conclusions

The flow patterns of a confined jet with and without target for high and low Reynolds numbers have been successfully visualized. The obtained photographs can be used to interpret not only the measurements but also help to enhance the physical insight of the flow mechanism. The flow visualization compliment the measurements by using hot-wire which either cannot reach the locations very near to the back wall or will cause an obstruction to the exit (located at the back wall) has hindered the study of the flow field at the region. (Note that the hot-wire measurement ended at x/d=30mm [5,6]). The flow visualization results suggested that it might be required to have a non-invasive measuring instrument such as Laser Doppler Anemometer to measure the flow field close to the back wall.

Acknowledgment

The financial support of the NTU ARP research grant RG 15/95 is gratefully acknowledged. The first author also likes to express his sincere thanks to Mr. P.G.C. Koh for taking the photographs of the flow visualization.

Nomenclature

d slot width

L mean velocity half width

Re Reynolds number ($U_j d/\nu$)

U mean axial velocity

U_j velocity at the jet exit

U_o local mean centerline velocity

x axial distance from nozzle exit

y lateral distance

ν kinematic viscosity

References

1. S. Honda and H. Yamasaki, A new hydrodynamic oscillator type flow meter, *Proc. of Int. Symp. on Fluid Control & Meas.*, Tokyo, **2,** 623 (1986).

2. A.C. Lua, K.S. Wee, W.K. Chan and C.Y. Liu, Target fluidic flowmeter with back walls for the flow recirculation, *Proc. of FLUCOME '94*, Toulouse, France, 2, 889 (1994).

3. A. Krothapalli, D. Baganoff and K. Karamcheti, On the mixing of a rectangular jet, *J. Fluid Mech*, **107**, 210 (1978).

4. L. P. Chua and R.A. Antonia, Turbulent Prandtl number in circular jet, *Int. J. Heat Mass Transf.*, **33**, 331 (1990).

5. L. P. Chua and A. C. Lua, Measurements of a confined jet, *Phys. of Fluids*, **10**, 3137 (1998).

6. L. P. Chua, A. C. Lua and H-S Li, *Proc.3rd ASME/JSME Joint Fluids Engg. Conference*, FEDSM **99-7040**, 1 (1999).

Received September 10, 1999